

# Spinning eggs — a paradox resolved

An explanation for an odd egg performance is rolled out in time for Easter.

If a hard-boiled egg is spun sufficiently rapidly on a table with its axis of symmetry horizontal, this axis will rise from the horizontal to the vertical. (A raw egg, by contrast, when similarly spun, will not rise.) Conversely, if an oblate spheroid is spun sufficiently rapidly with its axis of symmetry vertical, it will rise and spin about the vertical on its rounded edge with its axis of symmetry now rotating in a horizontal plane. In both cases, the centre of gravity rises; here we provide an explanation for this paradoxical behaviour, through derivation of a first-order differential equation for the inclination of the axis of symmetry.

The behaviour of these spheroids shows similarities to that of the mushroom-shaped top (known as the tippe-top) that has been previously analysed<sup>1–3</sup>; however, there are also significant differences that arise from the geometry of the general axisymmetric body. The essential mechanism can be traced to the action of the frictional force between the spinning object and the table. If this frictional force vanishes, or if the body rolls without slipping, the ‘rise’ phenomenon does not occur. Weak friction associated with slipping at the point of contact causes a secular instability, which gives rise to the surprising behaviour that is observed. (A fuller discussion of the subtleties involved is in preparation.)

The geometry and notation for the problem are shown in Fig. 1. We seek to obtain an equation for the polar angle,  $\theta(t)$ , between  $Oz$  and  $OZ$ . We adopt a rotating frame of reference  $OXYZ$ , with  $OX$  horizontal in the plane  $\Pi$  and  $OY$  into the plane of the diagram. The angular velocity of the body,  $\omega$ , has components in this frame

$$\begin{aligned}\dot{\omega} &= ((n - \Omega \cos \theta) \sin \theta, \dot{\theta}, \\ &\quad \Omega \sin^2 \theta + n \cos \theta)\end{aligned}\quad (1)$$

where  $n(t)$  is the spin (that is, the component of  $\omega$  about  $Oz$ ), and the dot represents time-differentiation. The angular momentum,  $\mathbf{H}$ , has components

$$\begin{aligned}\mathbf{H} &= ((Cn - A\Omega \cos \theta) \sin \theta, A\dot{\theta}, \\ &\quad A\Omega \sin^2 \theta + Cn \cos \theta)\end{aligned}\quad (2)$$

where  $A$ ,  $A$  and  $C$  are the principal moments of inertia at  $O$ . The height,  $h(\theta)$ , of  $O$  above the table is determined as a function of  $\theta$  from the geometry and density distribution of the body. The components of the vector  $\mathbf{X}_p = (X_p, 0, Z_p)$  from  $O$  to the point of contact,  $P$ , are then given by

$$X_p = dh/d\theta, Z_p = -h(\theta)\quad (3a, b)$$

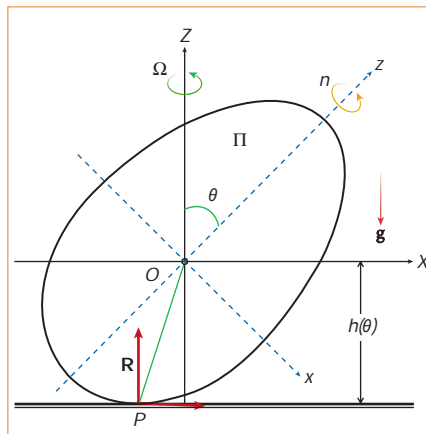


**Figure 1** An axisymmetric body with centre of mass  $O$  spins on a horizontal table with point of contact  $P$ . Its axis of symmetry,  $Oz$ , and the vertical axis,  $OZ$ , define a plane  $\Pi$  (containing  $OP$ ), which precesses about  $OZ$  with angular velocity  $\Omega(t) = (0, 0, \Omega)$ .  $OXYZ$  is a rotating frame of reference, with  $OX$  horizontal in the plane  $\Pi$ . The height of  $O$  above the table is  $h(\theta)$  and the coordinates of  $P$  are  $X_p = dh/d\theta$ ,  $Y_p = 0$ ,  $Z_p = -h(\theta)$ . The forces acting on the body are its weight  $Mg = (0, 0, -Mg)$ , the normal reaction  $\mathbf{R}$  at  $P$ , and the frictional force  $\mathbf{F}$  at  $P$  in the  $Y$ -direction.

If the frictional force vanishes, the horizontal velocity components of  $O$  may be taken to be zero (as no horizontal force then acts on the body). The slip velocity of the point  $P$  is then  $\mathbf{U}_p = (-h\dot{\theta}, V_p, 0)$ , where

$$V_p = (\Omega \sin^2 \theta + n \cos \theta) dh/d\theta + (n - \Omega \cos \theta) h(\theta) \sin(\theta)\quad (4)$$

In any steady state,  $\mathbf{U}_p = 0$ . When the frictional force is weak,  $\dot{\theta}$  is correspondingly small (as may be verified retrospectively), and at leading order,  $\mathbf{U}_p = (0, V_p, 0)$ . The frictional force,  $\mathbf{F}$ , tends to resist slipping; it follows that at leading order,  $\mathbf{F} = (0, F, 0)$ , where  $F$  is a function of  $V_p$  given by the law of dynamic friction between the two surfaces in contact. There is also a normal reaction  $\mathbf{R} = (0, 0, R)$  at  $P$ , where  $R$  is of order  $Mg$ .

Euler's angular-momentum equation is

$$d\mathbf{H}/dt + \Omega \times \mathbf{H} = \mathbf{X}_p \times (\mathbf{R} + \mathbf{F})\quad (5)$$

the right-hand side representing the torque exerted on the body relative to  $O$ . The  $Y$ -component of this equation is

$$\begin{aligned}A\ddot{\theta} - A\Omega^2 \cos \theta \sin \theta + Cn \Omega \sin \theta \\ = -RX_p\end{aligned}\quad (6)$$

Now  $|\ddot{\theta}| \ll \Omega^2$ , because the secular change of  $\theta$  with which we are concerned is slow; hence the first term of equation (6) may be neglected. Moreover, we shall sup-

pose, for simplicity, that  $\Omega^2$  is sufficiently large that the terms that involve  $\Omega$  in equation (6) dominate the term  $-RX_p$ . The precise condition for the case of uniform spheroids is given below (condition (14)). Thus, at leading order, equation (6) becomes simply  $(Cn - A\Omega \cos \theta) \Omega \sin \theta = 0$ , and so, provided that  $\sin \theta \neq 0$ ,

$$Cn = A\Omega \cos \theta\quad (7)$$

a condition that we may describe by the term ‘gyroscopic balance.’ In adopting this approximation (which is analogous to the geostrophic approximation in fluid mechanics), oscillatory modes of high frequency ( $O(\Omega)$ ) are filtered from the system. Using equation (7), the angular momentum (equation (2)) is simplified to  $\mathbf{H} = (0, A\dot{\theta}, A\Omega)$ .

The  $Z$ - and  $X$ -components of equation (5) now give, respectively,

$$A\dot{\Omega} = FX_p, A\Omega\dot{\theta} = FZ_p\quad (8a, b)$$

from which we can immediately obtain

$$\dot{\Omega}/\Omega = (X_p/Z_p)\dot{\theta} = -\dot{h}/h\quad (9)$$

using equation (3). This integrates to give  $\Omega h = \text{cst.}$ , or equivalently,

$$-\mathbf{H} \cdot \mathbf{X}_p = A\Omega h = J\quad (10)$$

where  $J$  is a constant determined by the initial conditions. This ‘Jellett’ constant has been found previously<sup>4</sup> for the particular case of bodies (such as the tippe-top) on the assumption that the portion of the surface in contact with the plane is spherical. The above derivation shows that the constant still exists quite generally as an ‘adiabatic invariant’ under the gyroscopic-balance condition (7) for the case of the general axisymmetric body. From equations (4), (7) and (10),  $V_p$  is now known as a function of  $\theta$ ; this may be expressed compactly as

$$V_p = (J/A)\zeta^{-3}h^{-1}d(\zeta h)/d\theta\quad (11)$$

where  $\zeta(\theta) = (\sin^2 \theta + (A/C)\cos^2 \theta)^{-1/2}$ .

Substituting equations (3b) and (10) into equation (8b) now gives

$$J\dot{\theta} = -Fh^2(\theta)\quad (12)$$

If the frictional relationship between  $F$  and  $V_p$  is known, and if  $h(\theta)$  is known through geometrical considerations, then equation (12) may be integrated to determine  $\theta$  as a

function of  $t$ . A steady state can be attained only when  $V_p=0$  (and so  $F=0$ ), because only then does the energy dissipation due to friction at  $P$  vanish.

For example, suppose that the body is the uniform spheroid  $a^2(x^2+y^2)+b^2z^2=a^2b^2$ . The principal moments of inertia at its centre,  $O$ , are  $A=M(a^2+b^2)/5$  and  $C=2Mb^2/5$ . The function  $h(\theta)$  is easily determined in the form  $h(\theta)=(a^2\cos^2\theta+b^2\sin^2\theta)^{1/2}$ , and from equation (11) we obtain the remarkable simplification

$$V_p=-(J/4Ah^2)(a^2-b^2)\sin 2\theta \quad (13)$$

Gyroscopic balance occurs provided that

$$\Omega^2 \gg \frac{5g|a^2-b^2|}{(a^2+b^2)\min(a,b)} \quad (14)$$

As regards the frictional force, there are two obvious possibilities. First, we may assume a Coulomb law,  $F=-\mu MgV_p/|V_p|$ ; then equation (12) integrates to give

$$\tan\theta=-(a/b)\tan\mu q(t-t_0) \quad (15)$$

where  $q=Mgab(a-b)/|a-b||J|$  and  $t_0$  is a constant of integration. Here we may take  $J=A\Omega^*((a^2+b^2)/2)^{1/2}$ , where  $\Omega^*$  is the value of  $\Omega$  when  $\theta=\pi/4$ . For the prolate spheroid ( $q>0$ ), this describes a monotonic decrease of  $\theta$  from  $\pi/2$  to 0 over the time interval  $[t_0-\pi/2\mu q, t_0]$ ; for the oblate spheroid ( $q<0$ ), it similarly describes a monotonic increase of  $\theta$  from 0 to  $\pi/2$  over the time interval  $[t_0, t_0+\pi/2|\mu q|]$ . In either case, equation (15) thus represents a transition from the unstable to the stable state over a finite time interval  $\Delta t=\pi/2|\mu q|$ .

Alternatively, if we assume a 'viscous'

friction law  $F=-\mu MgV_p$ , then equation (12) becomes  $\dot{\theta}=-(\mu q/2)\sin 2\theta$ , where now  $q=5g(a^2-b^2)/2(a^2+b^2)$ . This integrates to give

$$\tan\theta=e^{-\mu q(t-t_0)} \quad (16)$$

which again describes monotonic transition from unstable to stable states (whether  $q>0$  or  $q<0$ ) on the secular time scale  $|\mu q|^{-1}$ . Numerical integration of the exact equations (without use of the gyroscopic approximation) confirms the validity of this description.

The key to the above analysis lies in the fact that the Jellett constant (equation (10)) exists for arbitrary bodies of revolution as an adiabatic invariant when the condition described by equation (7) is satisfied, and not only for the previously analysed bodies with part-spherical forms.

Finally, we may note that a raw egg does not rise when spun, simply because the angular velocity imparted to the shell must diffuse into the fluid interior; this process dissipates most of the initial kinetic energy imparted to the egg, the remaining energy being insufficient for condition (14) to be satisfied and for the state of gyroscopic balance to be established.

**H. K. Moffatt\*, Y. Shimomura†**

\*Department of Applied Mathematics and Theoretical Physics, Silver Street, Cambridge CB3 9EW, UK  
e-mail: hkm2@damtp.cam.ac.uk

†Department of Physics, Keio University, Hiyoshi, Yokohama 223-8521, Japan  
e-mail: yutaka@phys-h.keio.ac.jp

Competing financial interests: declared none.

with a small, solitary cartilaginous condensation<sup>4</sup> (Fig. 1a).

To investigate whether modulation of *Hox*-gene expression in the mandibular arch could be associated with the evolutionary origin of jaws, I cloned lamprey *Hox* genes and analysed their expression patterns during embryogenesis. Two overlapping genomic cosmids (MPMGc055I1883 and MPMGc055J22138) were found to contain three *Hox* genes with orthology to the *Hox5-6-7* cognate group. During lamprey embryogenesis, the *HoxL6* (GenBank accession no. AY089982) expression domain spreads anteriorly from the blastopore and extends into the cranial mesoderm (see supplementary information), where I detected transcripts from the onset of mandibular-arch formation prior to colonization of this region by neural-crest cells<sup>9</sup> (Fig. 1b).

*HoxL6* continues to be expressed strongly in the mandibular and posterior arches as these become individually defined (Fig. 1c), and in two stripes in the dorsal hindbrain (see supplementary information), where the neural crest originates<sup>7-9</sup>. In older embryos, *HoxL6* expression was detected within each pharyngeal arch, and in the upper and lower lips (Fig. 1d). *HoxL6* transcripts co-localize with *Dlx*, a marker of the lamprey cranial neural crest<sup>10,11</sup>, and were later detected in hypertrophic chondrocytes, indicating that *HoxL6* is expressed by neural-crest cells in the pharyngeal arches (compare Fig. 1d and e, and see supplementary information).

Within the mandibular arch, however, I detected *HoxL6* transcripts and *Dlx* protein in mutually exclusive ventral and dorsal domains, respectively (Fig. 1d, e). Comparison of *HoxL6* and *HoxL5* (GenBank accession no. AY089981) expression revealed that the *HoxL6* domain extends anterior to the boundary of *HoxL5* expression (see supplementary information), suggesting that spatial collinearity<sup>12</sup> has been broken. These findings identify lampreys as the only known vertebrate in which *Hox* genes are expressed in the mandibular arch.

To determine whether the breakage of *Hox6* collinearity is a derived condition of lampreys, I analysed expression of the single *Hox6* orthologue *AmphiHox6* in the cephalochordate amphioxus. *AmphiHox6* expression was detected throughout the neural tube, up to the base of the cerebral vesicle, and in endoderm up to the first gill slit (Fig. 1f). *AmphiHox6* expression extends anterior to the *AmphiHox3* and *AmphiHox4* domains<sup>12</sup> and, like *AmphiHox2*, does not respect spatial collinearity. Thus, in cephalochordate and lamprey embryos, *Hox6* genes are expressed anterior to their 3' neighbours, indicating that this could be a general feature of non-

## Evolutionary biology

### Lamprey *Hox* genes and the origin of jaws

The development of jaws was a critical event in vertebrate evolution because it ushered in a transition to a predatory lifestyle, but how this innovation came about has been a mystery. In the embryos of jawed vertebrates (gnathostomes), the jaw cartilage develops from the mandibular arch, where none of the *Hox* genes is expressed; if these are expressed ectopically, however, jaw development is inhibited<sup>1-3</sup>. Here I show that in the lamprey, a primitive jawless (agnathan) fish that is a sister group to the gnathostomes<sup>4</sup>, a *Hox* gene is expressed in the mandibular arch of developing embryos. This finding, together with outgroup comparisons, suggests that loss of

*Hox* expression from the mandibular arch of gnathostomes may have facilitated the evolution of jaws.

In gnathostome embryos, cranial neural-crest cells migrate from the overlying mid- and hindbrain into the pharyngeal arches<sup>5,6</sup>, where they give rise to the pharyngeal skeleton, including the jaw. With the exception of those destined for the mandibular arch, cranial neural-crest cells express specific combinations of *Hox* genes, which reflect their site of origin in the segmented hindbrain<sup>5,6</sup>. In lamprey embryos, the branchial skeleton also develops from cranial neural-crest cells<sup>7,8</sup> but, in contrast to gnathostomes, the lamprey mandibular arch fails to form separate dorsal and ventral cartilage condensations<sup>4,9</sup>. Instead of forming a Meckel's cartilage, the lamprey first arch forms the velum, a muscular pumping organ